Photoemission Studies of Cesium Telluride[*]

R. A. Powell, W. E. Spicer, G. B. Fisher[†], and P. Gregory

Stanford Electronics Laboratories, Stanford University, Stanford, California 94305

(Received 8 January 1973)

Photoemission measurements have been made at photon energies from 3 to 12 eV on Cs_2Te films at pressures less than 5×10^{-10} Torr. Inelastic electron-electron scattering and electron-phonon scattering have a dramatic effect on the photoemission data. By using the three-step model of photoexcitation, hot-electron transport, and escape to describe photoemission in Cs_2Te, both the quantum yield above the main threshold and the energy distributions of photoemitted electrons (EDC's) can be qualitatively understood. Important features in the band structure Cs_2Te have also been deduced from the behavior of structure in the EDC's. Three maxima in the conduction-band density of states are located at 4.05 ± 0.1, 4.9 ± 0.1, and 5.4 ± 0.1 eV above the top of the valence band. Two peaks observed in the valence-band density of states at 0.7 ± 0.1 and 1.4 ± 0.1 eV below the top of the valence band have been assigned to the spin-orbit-split $5p$ orbitals of Te. The value for the spin-orbit splitting $(0.65 \pm 0.1$ eV) is in excellent agreement with the theoretical free-atom value. In addition, an upper bound of 2 eV was set for the over-all width of the valence band in Cs_2Te. Cs_2Te films overcoated with 5% additional Te were also studied. Both these films and the Cs_2Te films prepared without additional Te display a low yield ($\lesssim 10^{-5}$ electrons/incident photon) below the main threshold of the quantum yield. It was found that this low yield cannot be explained in terms of a simple excess of Cs or Te in an otherwise stoichiometric single-phase compound.

I. INTRODUCTION

Because of its lack of sensitivity to visible light and high photoelectric yield in the ultraviolet (uv), [1] Cs_2Te has been used for many years as a practical photocathode in photodiodes and photomultiplier tubes[2] and has recently been developed into a standard for uv light intensity. [3] In spite of this, its band structure and optical properties remain relatively unexplored. In this paper we report on recent photoemission studies of Cs_2Te in which the quantum yield and energy distribution curves (EDC's) of the photoemitted electrons were measured over a wide range of photon energies. The EDC's are of particular interest because the valence band width in Cs_2Te was found to be only about one-half the size of the band gap. As a result, a clear distinction can be made between the electrons which escape with little or no energy loss and those which have been scattered with large inelastic loss. That is, these two components of the EDC's are well separated in energy so that there is no difficulty in distinguishing between them.

Interpreting the photoemission from Cs_2Te, we find the three-step model[4] to be quite applicable. In this model, electrons are first optically excited into higher unfilled energy states. These hot electrons then migrate to the solid surface with or without scattering and, if they have sufficient energy, escape across the surface potential barrier into vacuum. As a result, measurements of the quantum yield and of the EDC's can be used to study both the optical-excitation processes and hot-electron transport in solids.

II. EXPERIMENTAL PROCEDURE

Samples were prepared using methods already developed in this laboratory for the production of stable high-yield Cs_2Te photodiodes. [3] (A discussion of standard techniques used to form Cs_2Te cathode films will be found in Ref. 2, p. 179.) These methods are based on the fact that at elevated temperatures ($\gtrsim 100$ °C) Cs vapor is known to react with Te to form the pale greenish semiconductor Cs_2Te. [5] First, spectroscopic grade Te (99.999% pure) was vapor deposited from a quartz-bucket evaporator onto a heat-cleaned polished Mo or Pt substrate held at room temperature. During evaporation, the main chamber pressure rose to slightly below 10^{-9} Torr. The Te films were polycrystalline as determined by x-ray analysis and were typically $\simeq 1200$ Å thick as measured using a quartz-crystal thickness monitor. Then, with the substrate held near 150 °C, the high-vacuum pumps were turned off and a glass ampoule containing about 1 g of Cs (99.98% pure) was broken in an annealed-copper side arm. The Cs vapor pressure in the main chamber was maintained at $\simeq 10^{-7}$ Torr by controlled heating of the side arm. Exposure to a Hg arc lamp during cesiation allowed the substrate photocurrent to be monitored as the reaction progressed. The photocurrent was observed to rise from 1×10^{-10} A to a maximum of 3×10^{-7} A and then to decrease with further (i. e., excess) cesiation. When the photocurrent fell to 50% of its maximum value, cesiation was stopped, the high-vacuum pumps turned back on, and the photocurrent rose gradually to near its maximum value. Annealing at 150 °C for 1 h and slow cooling completed the
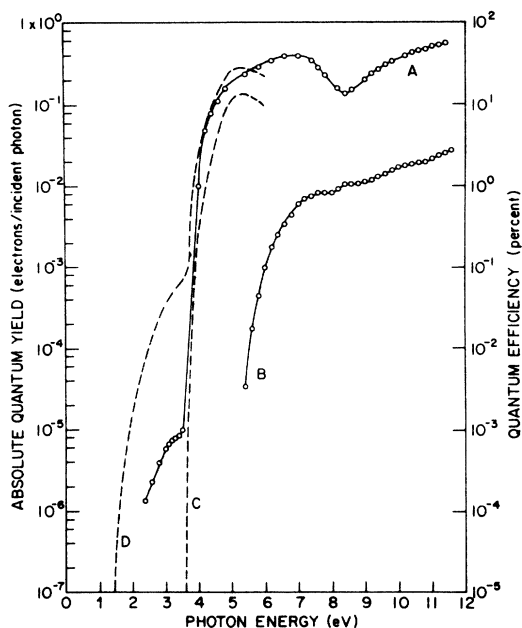
FIG. 1. Spectral distribution of the photoelectric yield from (A) Cs_2Te; (B) evaporated Te before reaction with Cs. Also shown are the data of Taft and Apker (Ref. 1). In their work, curve C was reported to be from a surface containing excess Cs while curve D was exposed to less Cs.

sample preparation. The resulting Cs_2Te films displayed a pale greenish yellow cast.

Subsequent photoemission measurements were carried out *in situ* at pressures less than 10^{-10} Torr. The sharp lines of a Hg arc discharge lamp were used at photon energies at the range $2 < \hbar\omega < 5$ eV, while for $\hbar\omega > 5$ eV a Hinteregger-type discharge lamp with a source gas of Hydrogen was employed. In the ultrahigh-vacuum chamber, the uv radiation must pass through a LiF window which does not transmit the radiation above 12 eV. Hence, no photoemission measurements were made for $\hbar\omega > 12$ eV.

III. PHOTOEMISSION STUDY OF Cs_2Te

A. Quantum Yield

In Fig. 1 we present the spectral distribution of the quantum yield for Cs_2Te which were measured using the absolute response of a calibrated Cs_3Sb phototube. For comparision, the previous measurements of Taft and Apker[1] are also presented. Before reacting with Cs, the Te film had a high photoelectric threshold near 5.0 eV as shown in Fig. 1 and a peak quantum yield of only about 3%. After the reaction, the threshold had dropped to about 3.5 eV and the peak quantum yield had risen to over 60% by $\hbar\omega = 11$ eV.

Between 3 eV and threshold, a one-half volt-wide shoulder appears. This shoulder was ob-

served in all Cs_2Te samples studied and has also been observed in the yields of Cs_2Te phototubes.[3] As mentioned in the Introduction, Cs_2Te combines a high sensitivity to uv radiation with a lack of sensitivity to visible radiation. This has made it particularly useful in astronomical uv observations where one wishes to avoid the detection of visible radiation from the sun or higher-order reflections from a grating. For such applications it is important to minimize the shoulder (Fig. 1). For many years, it was believed that the shoulder was due to excess Cs; however, in activating close-spaced Cs_2Te diodes, it has recently been found that the shoulder was reduced by a prolonged exposure to Cs and subsequent baking.[3] This procedure consistently gives shoulders of about 10^{-5} electrons/incident photon, whereas much higher shoulders have been reported (see curve D of Fig. 1). To further investigate the origin of this shoulder, a layer of Te (50 Å thick) was deposited onto the Cs_2Te surface. In Fig. 2 the yield obtained after this treatment is presented. The uv yield exhibits a much more uniform spectral response than that found in Cs_2Te films prepared without this additional Te deposit (Fig. 1); however, the peak quantum yield is now only about 10%, a decrease by a factor of 6. The low-energy shoulder is also reduced by almost an order of magnitude over that observed in the Cs_2Te samples prepared without additional Te. For comparison, the spectral response of an
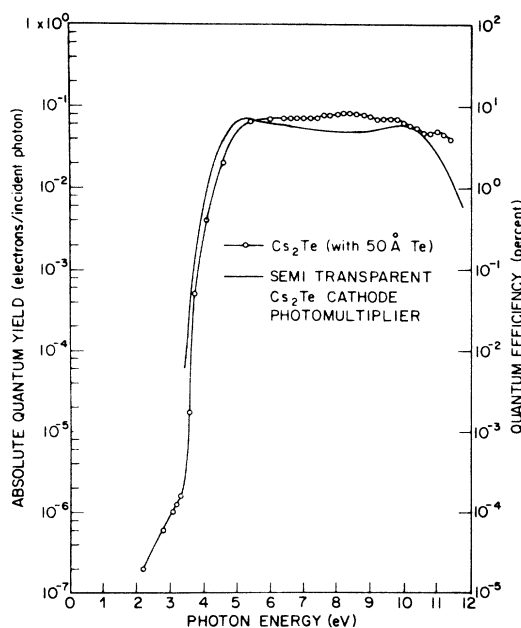

FIG. 2. Spectral distribution of the photoelectric yield from Cs_2Te overcoated with 50 Å of Te. Also shown is the the spectral response of an EMR photomultiplier which employs a semitransparent Cs_2Te cathode on a LiF window (Ref. 6).

SECONDARY
EMISSION
POSSIBLE

VACUUM

e-e SCATTERING
POSSIBLE

CONDUCTION
BAND $E_G + E_T$

$2E_G$

E_C

E_A E_{VAC}

E_G E_T
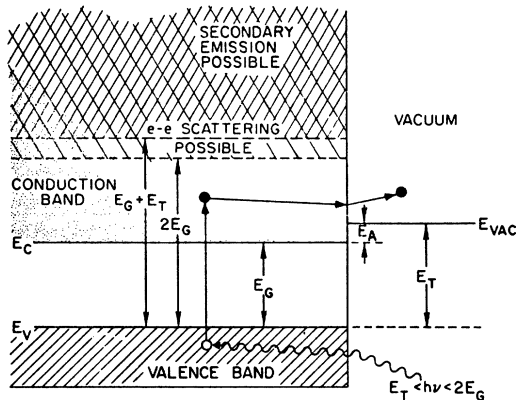
E_V

VALENCE BAND

$E_T < h\nu < 2E_G$

FIG. 3. Schematic energy-level diagram of a semi-conductor photoemitter where $E_G \gg E_A$. The minimum threshold energies for electron-electron scattering ($2E_G$) and for secondary electron emission ($E_G + E_T$) are indicated.

EMR photomultiplier[6] employing a semitransparent Cs_2Te cathode on a LiF window is also shown in Fig. 2. In the activation of these cathodes in practical tubes, the process is often finished by evaporating excess Te onto the Cs_2Te cathode in order to reduce emission below the threshold.

It appears then that the addition of 5% Te does not eliminate the shoulder although it does decrease it. This argues against the shoulder being simply due to a Cs excess in an otherwise stoichiometric, single-phase Cs_2Te film. If the film was single phase, the large Te addition should have produced much larger changes in the shoulder than were observed. The complex behavior of the shoulder and uv response with the Te addition, as well as the effect of Cs and long-term anneals, suggest that more than one phase of Cs_2Te may exist and that the shoulder as well as the uv yield are affected by this. The EDC's taken after the Te addition (see Appendix A) are consistent with this but not with a model which relates the shoulder below 4.0 eV to excess Cs or Te in an otherwise stoichiometric single-phase compound. Further study is clearly necessary to understand these phenomena.

The slope of the rising quantum yield above threshold is determined largely by the threshold escape function and the finite width of the valence band (VB). In Cs_2Te the yield displays an extremely pronounced rise (Fig. 1) increasing in one volt nearly four orders of magnitude over the value at 3.5 eV of less than 10^{-5} electrons/incident photon. Such a sharp threshold is indicative of a rather narrow VB. (It will later be seen that the over-all VB width in Cs_2Te is in fact only about 2 eV.) Above 4.5 eV, the yield continues to rise to a local maximum of about 40% for $\hbar\omega = 6.8$ eV, falls sharply to a local minimum near 8.3 eV, and rises again,

reaching about 60% by 11 eV. This behavior can best be understood in terms of the simple model shown in Fig. 3 and also discussed in Ref. 3. In this model the energy of the forbidden gap E_G and the threshold energy E_T differ only by the small electron affinity E_A (i.e., $E_G \gg E_A$, where $E_G + E_A = E_T$). Providing the electron energy is sufficiently large, inelastic electron-electron scattering (pair production) is the main energy-loss mechanism for the photoelectrons during transport to the surface and can have a dramatic effect on the photoemission data. In certain metals, for example, such pair production can limit the escape depth to about 10 Å or less.[7] Since the minimum energy that a primary electron can lose through pair production in a semiconductor is equal to the band gap energy E_G, pair production is not allowed for photon energies $\hbar\omega < 2E_G$. The escape depth may then be several hundred angstroms, limited only by electron-phonon scattering. Consequently, in this energy region, the model predicts a high quantum yield. Because of the narrowness of the VB in Cs_2Te, one would then expect a large yield before the escape depth is reduced by the onset of pair production. Since the band gap of Cs_2Te is near 3.0 eV, the threshold for pair production would then be near $\hbar\omega \simeq 6.0$ eV; however, owing to the increase in possible scattering events,[4] the probability for pair production rises from its threshold with increasing final-state energy and often only becomes large several eV above the threshold for pair production. In view of this, the drop off in yield beyond $\hbar\omega \simeq 7.0$ eV and the local minimum at 8.3 eV are assigned to the effects of the pair production. The local maximum observed in the yield at 7.0 eV can be thought of arising from a convolution of the rising quantum yield, expected in the absence of electron-electron scattering, with the decreasing probability of escape above $2E_G$, the threshold for pair production. The local maximum at 7.0 eV then indicates that the onset of pair production occurs at a somewhat lower photon energy in agreement with the band-gap value. For $\hbar\omega \gtrsim 6.8$ eV, the yield decreases rapidly with increasing photon energy, reflecting a corresponding decrease in the mean free path for electron-electron scattering above $\hbar\omega = 2E_G$. Initially, the scattered electrons fall below the escape threshold, dramatically reducing the yield; however, as photon energy increases, a point is reached for $\hbar\omega \geq E_G + E_T = 2E_G + E_A$ where the scattered primaries or secondaries have enough energy to escape. These electrons, however, being near threshold will not escape unless they are moving nearly perpendicular to the surface and therefore do not contribute noticeably to the yield. As $\hbar\omega$ increases, the number of electrons energetic enough to escape grows until by $\hbar\omega \simeq 8.3$ eV, the yield is finally observed to rise. It appears then
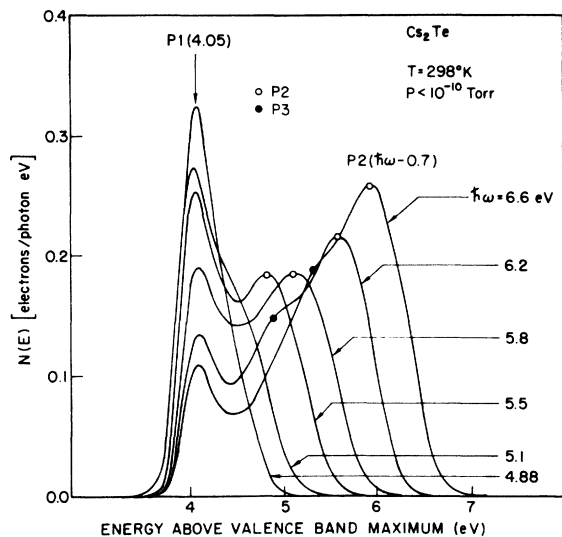
FIG. 4. Normalized energy distributions of the photo-emitted electrons $(4.88 \leq \hbar\omega \leq 6.6$ eV).

that the behavior of the yield can be qualitatively understood in terms of the onset of pair production near 6.8 eV. Measured EDC's, to be presented later in this paper, give additional support for this interpretation.

B. Energy Distribution of Photoemitted Electrons

In Figs. 4–6 we present selected EDC's for the photoemitted electrons measured using the ac-modulated retarding potential method of Spicer and Berglund[8] as improved by Eden.[9] All the EDC's have been normalized to the absolute quantum yield shown in Fig. 1. That is, the area under an EDC
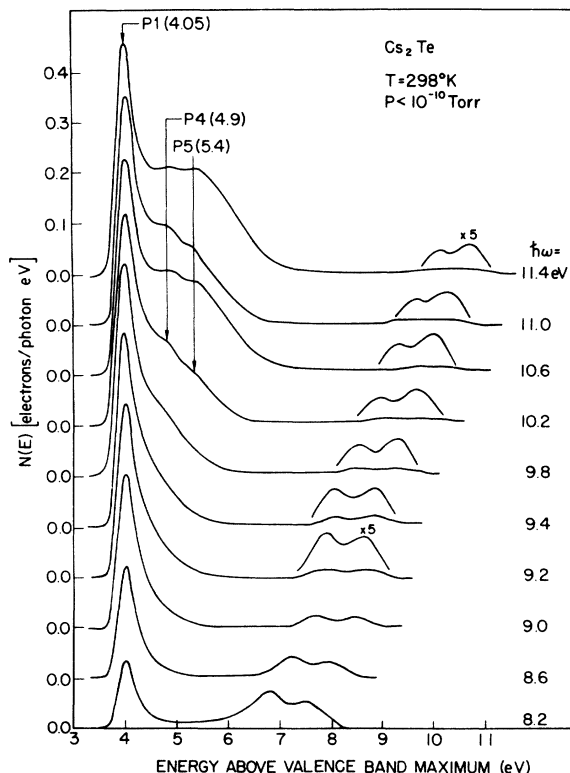

FIG. 6. Normalized energy distributions of the photo-emitted electrons $(8.2 \leq \hbar\omega \leq 11.4$ eV).

equals the measured yield at that photon energy. Electron energies are stated relative to the va-lence-band maximum (VBM) with an estimate un-certainty of ± 0.1 eV. It was also possible to ac-
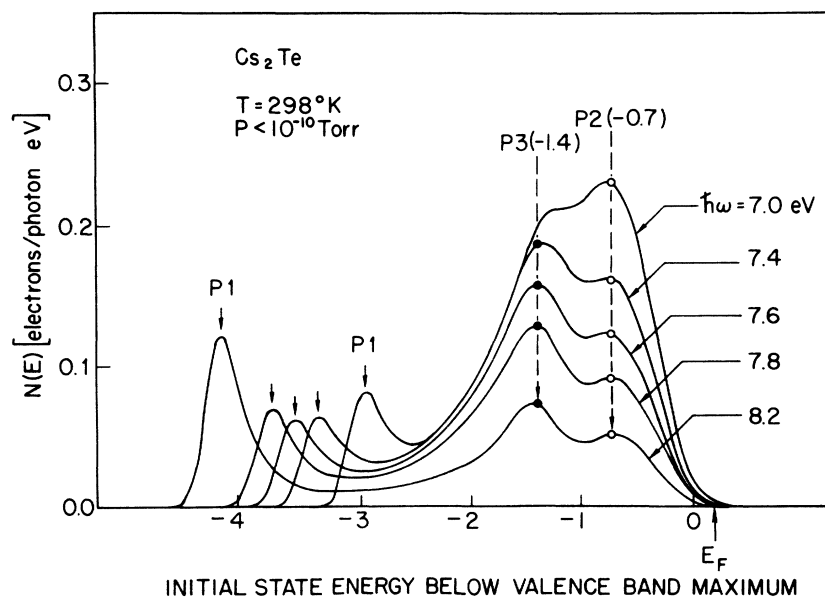

FIG. 5. Normalized energy distributions of the photoemitted electrons plotted with respect to initial state energies (7 $\leq \hbar\omega \leq 8.2$ eV).

curately determine the collector work function by withdrawing the Cs_2Te sample from the hemispherical collector can and taking EDC's instead from the copper-coated back shutter. Using this information, the Fermi level for our sample was placed about 0.2 eV above the VBM, revealing the semiconductor to be heavily p type.

As photon energy increases above threshold, the first feature to appear in the EDC's is the peak $P1$ (Fig. 4). $P1$ appears in all the EDC's taken and at the same final-state energy 4.05 eV. Since

$$E_{P1} = 4.05 \text{ eV} = \text{const} \tag{1}$$

we associate $P1$ with a maximum in the conduction-band density of states (CBDOS) lying 4.05 ± 0.1 eV above the VBM. The actual position of this maximum may lie somewhat lower but be obscured by the escape function. A second structure $P2$ appears in the EDC's for $\hbar\omega \gtrsim 5.1$ eV, whose strength increases with increasing photon energy. A corresponding decrease in the height of $P1$ occurs, so that by $\hbar\omega = 5.8$ eV, the two peaks are nearly equal in height. For all $\hbar\omega \gtrsim 5.5$ eV, the location of $P2$ is given very nearly by

$$E_{P2} = \hbar\omega - 0.7 \text{ eV}, \tag{2}$$

where E_{P2} is measured with respect to the VBM. We therefore associate $P2$ with a maximum in the valence-band density of states (VBDOS) located 0.7 ± 0.1 eV below the VBM.

In Figs. 4 and 5, the EDC's for $\hbar\omega \geq 6$ eV show a companion structure $P3$ which grows in strength with increasing photon energy until by $\hbar\omega = 7.4$ eV it is even stronger than $P2$. For all $\hbar\omega > 7$ eV, the location of $P3$ is very nearly given by

$$E_{P3} = \hbar\omega - 1.4 \text{ eV}. \tag{3}$$

We therefore associate $P3$ with a maximum in the VBDOS located 1.4 ± 0.1 eV below the VBM. It should be noted that not only are Eqs. (1)–(3) satisfied over a large energy range but that, once $P2$ and $P3$ are well above the vacuum level, the shape of the structure associated with these peaks does not change as $\hbar\omega$ is changed. The relative peak heights, however, do change as photon energy is changed. We discuss this effect in more detail in Sec. III C. The location of structures $P1$, $P2$, and $P3$ in the EDC's are in good agreement with similar features observed earlier by Taft and Apker[1] for $\hbar\omega < 6.8$ eV; however, no assignments were then made for these structures.

The behavior of the EDC's in Cs_2Te is similar to those in related materials such as Cs_3Sb and Cs_3Bi and suggests that conservation of $\vec{k}$ may not provide an important optical selection rule.[10] Because of this, the EDC's may be understood, at least to the first approximation, in terms of a nondirect model[11,12] in which the probability $\mathcal{P}(E, \hbar\omega)$

for a photon of energy $\hbar\omega$, optically exciting an electron to a final state energy E, is proportional to

$$\mathcal{P}(E, \hbar\omega) \propto N_f(E) N_i(E - \hbar\omega), \tag{4}$$

where $N_f(E)$ and $N_i(E - \hbar\omega)$ are the density of final and initial states, respectively. We will discuss the density of initial states obtained from this model later.

In addition to the optical excitation, one must include the effects of inelastic scattering in order to understand the EDC's. For example, one must take into account the onset of scattering of the optically excited electron (producing a secondary electron-hole pair) in order to understand the photoemission behavior for $\hbar\omega \geq 6.6$ eV (Figs. 1, 4, and 5). The onset of a pair production near 6.6 eV produces the rapid decrease of the quantum yield previously noted. This indicates then that $E_G \lesssim 3.3$ eV. In this energy range, high-energy electrons are photoemitted from the VB to the conduction band (CB) and scatter down in energy below or near threshold. Hence, peaks $P2$ and $P3$ are observed to diminish in strength (Fig. 5). The secondary electrons scattered up to the CB also have insufficient energy to escape in large numbers. Hence, the strength of $P1$ remains small and relatively constant. The pronounced growth of $P1$ in the EDC's for $\hbar\omega \geq 8.2$ eV (Figs. 5 and 6) indicate that the once-scattered primaries are being scattered down to the CBDOS maximum at 4.05 eV and have sufficient energy left to escape the crystal in large numbers. It should be emphasized that the occurrence of a CBDOS maximum at 4.05 eV is based on the behavior at lower photon energies. As can be seen in Fig. 4, there is a maximum in the EDC's when the valence electrons are directly excited, without inelastic scattering, into the CBDOS at 4.05 eV. In a wide variety of materials, the production of secondary electrons by multiple scattering is observed. The effect of the threshold function on this distribution of secondaries may then be to produce a peak in the EDC's near threshold, similar to $P1$, but without having invoked any density-of-states effects.[13] Is one therefore justified in interpreting the growth of $P1$ as electrons scattered down to CB structure at 4.05 eV? As stated above, the existence of the CBDOS maximum at 4.05 eV is based on the behavior of $P1$ in the EDC's at low photon energies (Fig. 4) well before the onset of multiple scattering effects.

The increase in the relative numbers of electrons involved in pair production can clearly be seen in the EDC's for $\hbar\omega \gtrsim 9.4$ eV (Fig. 6). These EDC's are particularly dramatic in that almost all of the electrons emerge with energies less than 5 eV. As a consequence, the quantum yield above 9 eV (see Fig. 1) must now be viewed as being almost entirely due to this slow group of once-scattered electrons. It is relatively easy to separate this pro-

nounced peak of slow-moving electrons from elec-
trons that were photoexcited to the CB and subse-
quently escaped the crystal without scattering.
These latter electrons produce a 2-V-wide distri-
bution that moves with photon energy away from P1
(Fig. 6).

Above $\hbar\omega \simeq 9.2$ eV, a shoulder begins to appear
on the high-energy side of the scattering peak P1,
and P1 itself begins to grow in amplitude. We at-
tribute this behavior to the appearance of scat-
tered primaries and secondaries produced by the
electron-electron scattering event. As $\hbar\omega$ is in-
creased, the edge of the shoulder moves to higher
energy as would be expected since the primary en-
ergy increases with $\hbar\omega$. Note that the strength of
the primary peaks, P2 and P3, decreases some-
what with increasing $\hbar\omega$ as would be expected, since
the electron-electron scattering normally increases
with increasing final-state energy.

Note that definite substructure develops in the
shoulder above P1. For $\hbar\omega \gtrsim 10.2$ eV, two peaks,
P4 and P5, are clearly resolved at final-state en-
ergies 4.9 and 5.4 eV, respectively. One would
expect this structure to be due to the final states
into which the electrons are scattering; however,
there was no evidence for such density-of-states
structure when P2 and P3 moved through the same
final-state energies (see Fig. 4). This difference
may be due to different matrix elements for the op-
tical excitation and scattering events.

C. Valence-Band Density of States

It was remarked earlier that the electrons which
escaped the crystal without large loss in energy due
to inelastic scattering produced a well defined 2-
V-wide distribution in the EDC's for $\hbar\omega \gtrsim 9$ eV (Fig.
6). This distribution moves with photon energy
away from the pronounced inelastic scattering peak
P1. Now, the optical transitions in Cs_2Te were
seen earlier to fit the nondirect model[11,12] [see Eq.
(4)]. If the CBDOS is nearly constant in the region
of final-state energies where this distribution ap-
pears, then, in the absence of electron-electron
scattering, the shape and width of this distribution
mirror the shape and width of the VBDOS.[14] Un-
fortunately, because of the strong electron-electron
scattering observed in Cs_2Te, the VB structure
seen in the EDC's is not an exact replica of the
true VBDOS. Although the *location* of structure
should be unaffected by pair production, one must
be rather careful in deducing *relative peak heights*
in the DOS from the EDC's. For example, in the
EDC's for $\hbar\omega < 7.0$ eV (Fig. 4), the strength of P2
exceeds that of P3; however, after the onset of
pair production for $\hbar\omega \gtrsim 7.0$ eV, the relative peak
heights are reversed (Fig. 5). The increase in
the cross section for electron-electron scattering
with increasing electron energy may be such that

more electrons scatter out of the P2 distribution
than from the P3 distribution, effectively revers-
ing the relative peak heights observed in the EDC's.
Obviously, the VBDOS undergoes no such reversal.
At higher photon energies $\hbar\omega \gtrsim 9.8$ eV (Fig. 6)
relative peak heights are once again reversed in
the EDC's. At such high final-state energies, the
electron-electron-scattering cross section is ex-
pected to be nearly energy independent.[4] Elec-
trons are then no longer scattered preferentially
out of the higher energy peak P2. Consequently,
we might expect the VBDOS derived from these
EDC's to closely approximate the true VBDOS in
the solid. However, without detailed knowledge
of how the inelastic cross section depends on elec-
tron energy we cannot be sure of the relative peak
heights in the VBDOS. Lacking this knowledge,
we have arbitrarily set the peak heights equal in
the experimentally determined VBDOS for Cs_2Te
shown in Fig. 7. Also indicated in the calculated
value of the free-atom spin-orbit splitting for Te
$(5p_{3/2} - 5p_{1/2})$.[15]

We suggest that the two peaks P2 and P3 repre-
sent the spin-orbit-split atomic $5p$ orbitals of Te.
Similar behavior involving Bi and Sb has been ob-
served in the VBDOS of both Cs_3Bi and Cs_3Sb.[10,11]
In theory, the multiplicity of the splitting in the
solid depends on the crystal symmetry; however,
the exact crystal structure of Cs_2Te is not known.
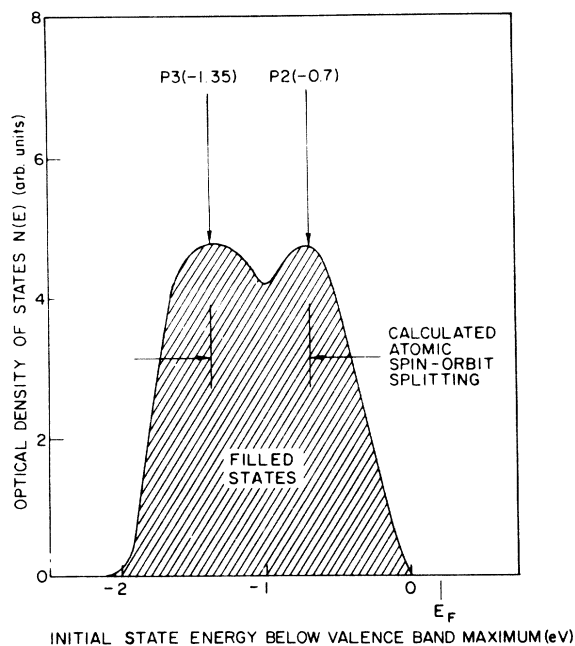

FIG. 7. Valence-band density of states in Cs_2Te as
determined from the experimental EDC's. Lacking the
exact energy dependence of the electron-electron-scat-
tering cross section, we have set the relative peak height
equal to unity.

In solids having cubic symmetry (e.g., Cs_3Bi and Cs_3Sb), the spin-orbit splitting should give rise to only two pwaks in the VBDOS. In addition, the spin-oribt splitting of the p states in cubic solids is often such that the higher lying states are doubly degenerate. [10] The presence of two peaks in the experimentally determined VBDOS suggests that Cs_2Te may be present in a cubic modification. In this case, we expect that the area associated with peak $P2$ would then be twice that associated with $P3$. Unfortunately, we were unable to verify this without the exact energy dependence of the inelastic scattering cross section as discussed above. However, as can be seen from Fig. 7, the experimental value (0.65 eV) for the splitting in the solid and the calculated free-atom value (0.68 eV) are in excellent agreement. [16] Such atomiclike behavior is not unexpected since a narrow VB ($\simeq 2.0$ eV) is indicative of a small Te-Te overlap. In the case of elemental Te, where the VB width is considerably larger than Cs_2Te, no such clear-cut evidence of spin-orbit-split structure is observed in the EDC's. [17,18]

One word of caution should be added regarding the VB width deduced in the preceding paragraphs. This should be regarded as an upper limit on the true VB width. As has been mentioned above, there is little evidence that the $\vec{k}$ conservation provides an important optical selection rule in Cs_2Te. This could be due to the valence hole produced in the optical-excitation process being localized for a time larger than the time for optical excitation at a given Te site. In such a case, lattice interaction could lead to appreciable broadening in the EDC's. A possible mechanism has been discussed previously. [12]

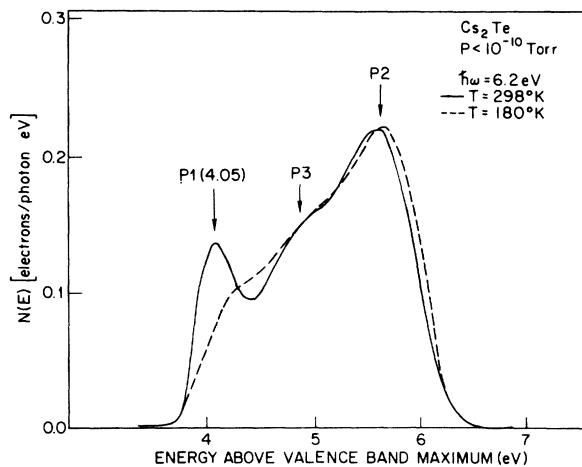In view of the rather narrow VB in Cs_2Te, it is necessary to reexamine the presence of $P1$ (4.05

FIG. 8. Normalized energy distributions of the photoemitted electrons for $\hbar\omega = 6.2$ eV at $T = 298$ and 180 °K.

TABLE I. Phenomena identified in quantum yield and EDC's of Cs_2Te.

Event	Photon energies for which observed	Corresponding features in EDC's and/or yield
Optical transitions to CBDOS maximum	$3.5 < \hbar\omega < 6.0$ eV	Stationary peak $P1$ (4.05 eV)
Optical transitions from VBDOS maxima	$\hbar\omega \gtrsim 5.1$ eV $\hbar\omega \gtrsim 6.0$ eV	Peaks $P2$ (−0.7 eV) and $P3$ (−1.4 eV) that move with photon energy (i.e., $\Delta E = \Delta \hbar\omega$)
Electron-phonon scattering	all values of $\hbar\omega$	Presence of $P1$ (4.05 eV) in the EDC's at these photon energies
Onset of inelastic electron-electron scattering	$\hbar\omega \gtrsim 7$ eV	Drop in the yield above 6.8 eV. Marked decrease of $P2$ and $P3$ in the EDC's
Escape of inelastically scattered primaries and secondaries due to pair production	$\hbar\omega \gtrsim 8.2$ eV $\hbar\omega \gtrsim 9.2$ eV	Increase of the yield above 8.3 eV. Growth of inelastic scattering peak $P1$. Broadening of $P1$ on the high-energy side with appearance of structures $P4$ (4.9 eV) and $P5$ (5.4 eV).

eV) in the EDC's for $6 < \hbar\omega < 7$ eV (Figs. 4 and 5). Direct photoexcitation into final states 4 eV above the VBM is forbidden because the initial states would then lie below the bottom of the VBDOS. In addition, at these low photon energies, the threshold for electron-electron scattering across the band gap has not yet been reached. Such scattered electrons could not then be responsible for $P1$ in this energy range. It is suggested instead that we are dealing with transitions involving inelastic phonon scattering. By losing energy through successive phonon scattering events in the CB, the photoexcited electrons could thermalize down to the CBDOS maximum near 4 eV. This is brought out more clearly in Fig. 8 in which we present EDC's taken for $\hbar\omega = 6.2$ eV at 298 and 180 °K. The average energy loss per electron-phonon scattering event is expected to be lower at the lower temperature and the events themselves may be less frequent. Hence, at $T = 180$ °K we expect that fewer electrons will lose sufficient energy to reach the CBDOS maximum before escaping the solid. Indeed, the strength of $P1$ is seen to be sharply reduced at the lower temperature and $P2$ appears at a slightly higher energy.

IV. CONCLUSIONS

In conclusion, then, photoemission measurements have been used to determine important features in the band structure of Cs_2Te. Three maxima in the CBDOS are located at 4.05 ± 0.1, 4.9 ± 0.1, and 5.4 ± 0.1 eV above the VBM. Two peaks observed in the VBDOS at 0.7 ± 0.1 and 1.4 ± 0.1 eV below the VBM have been associated with the spin-orbit-
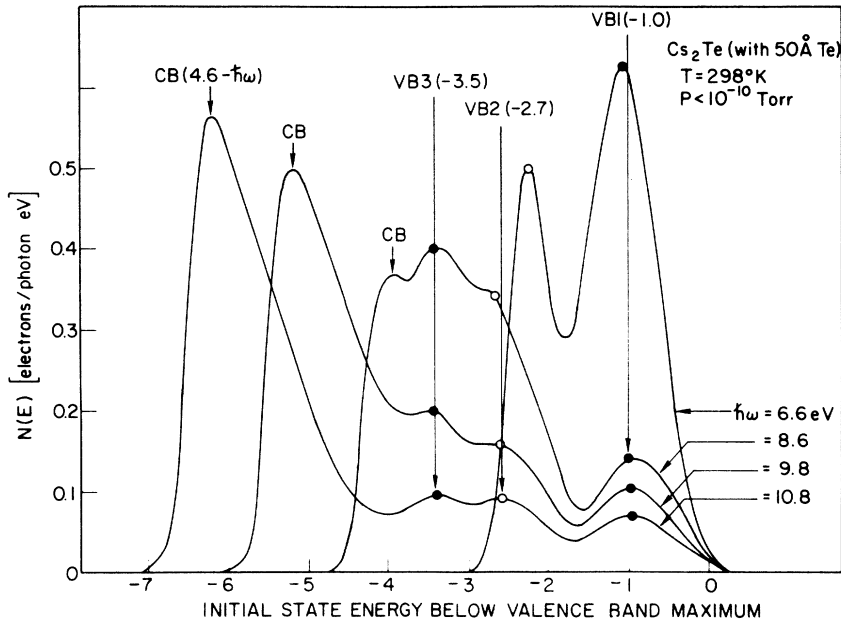
FIG. 9. Energy distributions of the photoemitted electrons from Cs_2Te overcoated with 50 Å of Te $(6.6 \leq \hbar\omega \leq 10.8$ eV).

split $5p$ orbitals of Te. In addition, an upper bound on the over-all width of the VB was set at 2.0 ± 0.2 eV. We tentatively assess the band gap to be $\lesssim 3.3$ eV. We consider these features a first approximation to the band structure of Cs_2Te. A more complete picture can best be obtained by considering experimental techniques in addition to photoemission. In this respect, measurements of the reflectivity and optical absorption from 3 to 12 eV would be of great value.

The source of the shoulder in the yield below 4.0 eV was reexamined and it was concluded that it could not be explained in terms of a simple excess of Cs or Te in an otherwise stoichiometric single-phase compound. Rather, it is suggested that more complex behavior such as a two-phased system is responsible for the shoulder. More work clearly needs to be done in order to resolve this problem.

In Table I we summarize phenomena identified in the quantum yield and EDC's of Cs_2Te. The necessity of introducing hot-electron transport to understand this data demonstrates the bulk nature of this photoemission and supports using the three-step model[4] of photoexcitation, transport, and escape to describe photoemission in Cs_2Te and related compounds with high photoelectric yields.

ACKNOWLEDGMENT

We appreciate the assistance of Neville Smith for providing us with the Cs ampoule.

APPENDIX A

In Fig. 9 several EDC's taken after the addition of 50 Å of Te are presented. These are of particu-

lar interest because of questions as to whether the shoulder in the quantum yield below 4.0 eV (see Sec. III A and Figs. 1 and 2) is due to a simple excess of Cs or Te in otherwise stoichiometric Cs_2Te.

The character of these EDC's can be seen to be quite different from that (see Figs. 4–6) found before the Te addition. The pronounced stationary peak CB appears to be an inelastic scattering peak representing a CBDOS maximum at 4.6 ± 0.1 eV above the VBM. The position of the remaining three structures, VB1, VB2, and VC3, move with photon energy (i.e., $\Delta E = \Delta \hbar\omega$) over a wide range of $\hbar\omega$. They therefore provide a rough picture of the VBDOS, indicating density of states (DOS) maxima at 1.0 ± 0.1, 2.7 ± 0.1, and 3.5 ± 0.1 eV below the VBM. As shown in Figs. 4–7, the Cs_2Te studied in this work has peaks at 0.7 and 1.4 eV below the VBM. Whatever its cause, this VBDOS is considerably different from that observed before the Te addition (see Fig. 7). It does not resemble the VBDOS observed in elemental Te,[17,18] which might have been the case had the sample remained heavily Te rich at the surface. Neither does it appear to be a composite of the VBDOS of Te and the Cs_2Te samples prepared without excess Te. Furthermore, after the Te addition, the Fermi level remained unchanged at about 0.2 eV above the VBM. Thus, it seems unlikely that the changes brought about by the Te addition can be explained simply in terms of excess Cs or Te in an otherwise stoichiometric single-phase system. On the other hand, there may be a relation between these effects and variations observed in the quantum yield of nonuniform cathodes.[3] In any event, the

EDC's of Fig. 9 are not understood in detail. As we mentioned in Sec. III A, more work is necessary before these phenomena can be completely understood.

*Work supported by NASA and NSF through the Center for Materials Research at Stanford University, Stanford, Calif.

†Present address: Division of Engineering, Brown University, Providence, R. I. 02912.

[1] E. Taft and L. Apker, J. Opt. Soc. Am. **43**, 81 (1953).

[2] A. H. Sommer, *Photoemissive Materials* (Wiley, New York, 1968).

[3] G. B. Fisher, W. E. Spicer, P. C. McKernan, V. F. Pereskok, and S. J. Wanner, Appl. Opt. **12**, 799 (1973).

[4] W. E. Spicer, Phys. Rev. **112**, 114 (1958); C. N. Berglund and W. E. Spicer, Phys. Rev. **136**, A1030 (1964).

[5] *Gmellins Handbuch der Anorganischen Chemie*, 8th. ed. (Verlag Chemie, Berlin, 1938), System No. 25, Caesium, p. 230.

[6] The photomultiplier quantum efficiency shown is EMR photomultiplier (Model No. 541F-08-18) of Electro-Mechanical Research, Inc., Princeton, N.J. The curve matches current specifications and is from J. A. Samson, *Techniques of Vacuum Ultraviolet Spectroscopy* (Wiley, New York, 1967), p. 225.

[7] N. V. Smith and G. B. Fisher, Phys. Rev. B **3**, 3662 (1971).

[8] W. E. Spicer and C. N. Berglund, Rev. Sci. Instrum. **35**, 1665 (1964).

[9] R. C. Eden, Rev. Sci. Instrum. **41**, 252 (1970).

[10] F. Wooten, J. P. Hernandez, and W. E. Spicer, J. Appl. Phys. **44**, 112 (1973).

[11] W. E. Spicer, Phys. Rev. Lett. **11**, 5291 (1963).

[12] W. E. Spicer, Phys. Rev. **154**, 385 (1967).

[13] C. N. Berglund and W. E. Spicer, Phys. Rev. **136**, A1030 (1964).

[14] N. B. Kindig and W. E. Spicer, Phys. Rev. **138**, A561 (1965).

[15] F. Herman and S. Skillman, *Atomic Structure Calculations* (Prentice-Hall, Englewood Cliffs, N.J., 1963).

[16] Band-structure effects are expected to increase the spin-orbit splitting observed in the solid over that of the free-atom value. Such effects are most pronounced at a region of high symmetry in the Brillouin zone (BZ), e.g., at the center of the zone where the DOS is small. However, transitions responsible for $P2$ and $P3$ have been associated with high VBDOS regions of the BZ, e.g., the zone faces. In these regions of low symmetry, band-structure effects are less important. In view of this, we might expect the spin-orbit splitting in Cs_2Te obtained from photoemission to be less than that obtained from, say, the fundamental optical absorption since the latter measurement probes states near the center of the BZ.

[17] L. D. Laude, B. Fitton, and M. Anderegg, Phys. Rev. Lett. **26**, 637 (1971).

[18] R. Powell and W. E. Spicer (unpublished).